

Spectroscopy of Random Two-Level Systems in Insulating Films

B. Sarabi,^{1,2} A. N. Ramanayaka,^{1,2} A. L. Burin,³ F. C. Wellstood,^{2,4} and K. D. Osborn^{1,4}

¹Laboratory for Physical Sciences, College Park, MD 20740, USA

²Department of Physics, University of Maryland, College Park, MD 20742, USA

³Department of Chemistry, Tulane University, New Orleans, LA 70118, USA

⁴Joint Quantum Institute, University of Maryland, College Park, MD 20742, USA

(Dated: June 16, 2022)

Using a calibrated uniform dc electric field, we modify the energy potential of randomly occurring two-level systems (TLSs) in an insulating film and probe them using a superconducting microwave resonator at millikelvin temperatures. This allows measurement of the excitation energies of *individual* TLSs dependent on the z -component of their electric dipole moment p_z . The hyperbolic energy dependence of TLSs reveals the state of double well degeneracy which allows for a precise measurement of p_z and the tunneling strength for each individual TLS. This method of degenerate well resonator (DWR) spectroscopy resolves multiple dipole types from a thick *insulating* film, and in silicon nitride we observe distinct types with maxima at $p_z = 3.3$ and 8.3 Debye. Sixty TLSs are measured with this technique, and the loss tangent microscopic observations is consistent with ensemble-averaged data. The TLS-resonator ac coupling is also measured and, with p_z , provides a quantum electrodynamical measurement of the vacuum fluctuation field. The same fluctuation field calculated from the electric field volume is only 16% smaller.

Dielectric two-level systems (TLSs) have attracted the attention of the superconducting quantum computing community ever since they were identified as a major cause of decoherence in superconducting qubits [1]. Subsequently, TLSs also became important to astronomers because they were found to be a performance-limiting source of noise in microwave kinetic inductance detectors (MKIDs) [2]. This motivation has led to quantum characterization of individual TLSs in the tunneling barrier of superconducting qubits and TLS-ensemble measurements of noise and quality factor in superconducting resonators. The TLSs are found in various dielectric structures including deposited insulating films [1, 3, 4], Josephson tunneling barriers [1, 5, 6], imperfect interfaces with crystalline substrates [7], and the native oxides of superconductors and substrates [8].

Measurements of *individual* TLSs with qubits (using TLS-qubit coupling) [1, 6, 9–11] and resonators (using TLS-resonator coupling, *i.e.* cavity quantum electrodynamics (CQED)) [12] are sensitive to the coherence of the TLSs. The former approach has measured individual TLSs in tunnel barriers with a thickness of ~ 2 nm, while the latter has measured individual TLSs in a 250 nm thick insulator. The microscopic structure and elemental composition of TLSs are generally unknown. However, recent modeling has predicted possible structures and TLS moments [13, 14].

The difficulty in identification is partially related to their random parameters. TLSs are generally characterized through a standard double-well minima model [15–17], in which each TLS is constructed from two wells with energy minima difference Δ , coupled to one another through a tunneling energy Δ_0 . A TLS has an excitation energy $\mathcal{E} = \sqrt{\Delta_0^2 + \Delta^2}$, and can be represented by a charge q and wells separated by \mathbf{d} within the solid, or a

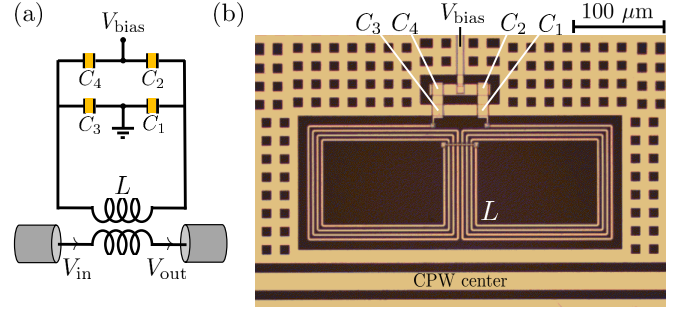


FIG. 1. (a) Schematic of the tunable micro-V resonator. (b) Optical image of the fabricated tunable micro-V resonator. Aluminum appears light and the sapphire substrate appears black.

dipole moment $\mathbf{p} \equiv q\mathbf{d}/2$.

In many individual TLS measurements the physical dipole moment p is unknown, but the ac coupling or the transition dipole moment $(\Delta_0/\mathcal{E})p|\cos\theta|$, where θ is the angle of \mathbf{p} with respect to the electric field, is extracted [18, 19]. TLS dipole moment measurements from individual moments in devices fall into three categories; (i) measurements with ac coupling only, (ii) measurements with ac coupling and dc electric field control and (iii) the bulk sample measurements. For the first type, statistics on the TLS transition dipole moments are used with the standard model distribution $dn \propto d\Delta_0/\Delta_0$ and the random distribution in θ , and with an assumption about the tunneling barrier thickness, the moment is extracted [1, 20]. In the second category a bias field \mathbf{E}_{bias} is used to sweep the TLS transition energies according to

$$\mathcal{E}' = \sqrt{\Delta_0^2 + (\Delta + 2\mathbf{p} \cdot \mathbf{E}_{\text{bias}})^2}, \quad (1)$$

while measuring the loss tangent [21]. This method has

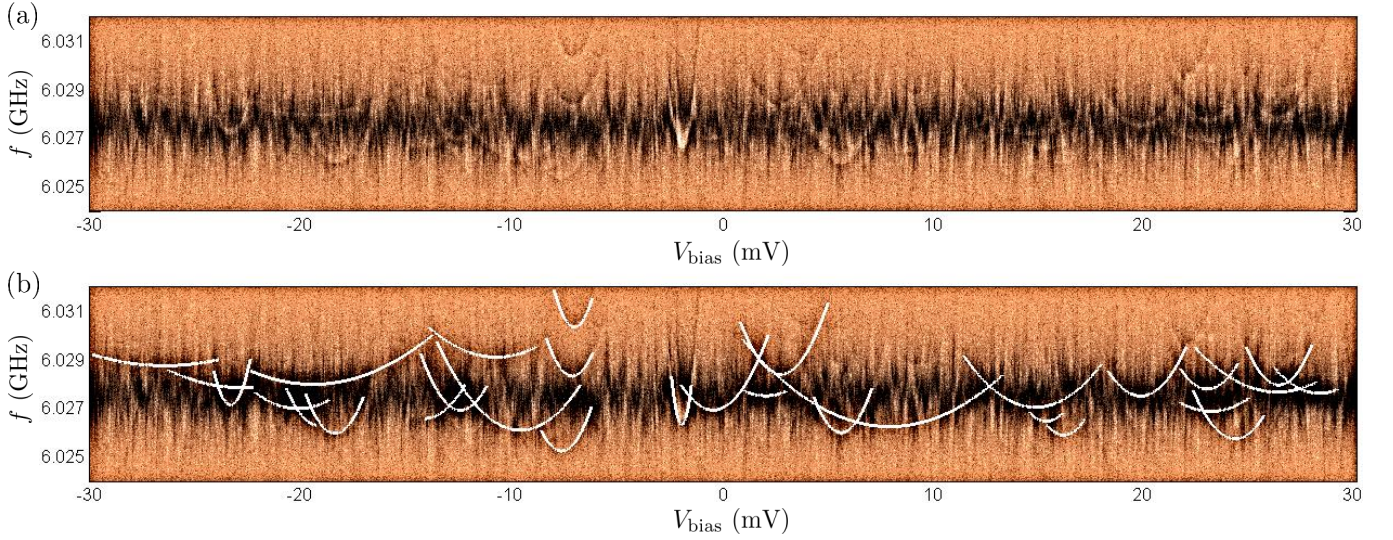


FIG. 2. (a) False-color plot of measured $|S_{21}|$ vs. frequency f and bias voltage V_{bias} . Data is taken at $T = 25$ mK and $\bar{n}_{\text{max}} \simeq 0.4$. Light copper and black correspond to $|S_{21}| = 0.56$ and $|S_{21}| = 0.40$, respectively. (b) Same data with overlaid fit to 30 hyperbolas.

only yielded one representative dipole moment, which is similar to the first type, but it is also accurate by comparison because the film thickness is relatively large and known. Finally, an early electric-echo measurement of bulk SiO_x has yielded a *single* (effective) dipole moment [22]. While these studies are interesting, they do not yet allow for the precise characterization of multiple TLS types in devices. The current work also uses electric field tuning similar to the second technique, but applies this field for static tuning. In this way, it is related to static strain tuning measurements of TLSs in tunneling barriers [23].

If a technique with enhanced precision were to measure multiple TLS dipole moments in dielectrics of superconducting circuits, one could classify the defects according to their deleterious phenomena, which would at least allow a reduction of these defects during fabrication. TLSs are often found in insulating structures without tunnel barriers but containing different insulating materials *e.g.*, capacitors, such that it is useful to explore relatively thick insulators. Aside from one exception [12], individual TLS studies have been limited to those within tunneling barriers made of aluminum oxide.

In this work, we measure *individual* TLSs in an *insulating* film while tuning their energy with a calibrated dc electric field aligned with the ac field. The ac field arises from a resonator that probes many TLSs near degeneracy, *i.e.* $\Delta_0/\mathcal{E} \simeq 1$. Hence we call our technique degenerate well resonator (DWR) spectroscopy. For each TLS double-well, $p_z = p|\cos\theta|$ is extracted from the tuned spectrum. This allows identification of multiple distinct TLS types in the film. In addition, a relatively fast exchange of a single excitation between the resonator and strongly coupled TLSs allows us to see CQED vacuum

fluctuation effects.

A superconducting resonator with an electrical bridge arrangement of parallel-plate capacitors was used, as shown in Fig. 1. The capacitor bridge isolates the dc bias voltage V_{bias} lead from coupling to the ac drive amplitude V_{in} and the ac resonance amplitude [21]. The device was fabricated on a sapphire substrate, and a $d_0 = 125$ nm thick PECVD silicon nitride (SiN_x) film sandwiched between two superconducting aluminum layers formed the capacitors. A quadrupole spiral inductor with the capacitors created a resonance frequency of approximately 6 GHz. The total SiN_x dielectric volume is $V = 78 \mu\text{m}^3$, and due to the small volume used we refer to this device as a tunable micro- V resonator. This dielectric volume hosts a few TLSs on average \bar{N} within the bandwidth B of the resonator, which allows detection of CQED effects. To get this number of TLSs, the dielectric used here had an approximately 7 times larger TLS density than an earlier device which did not employ tuning [12], and is understood to be related to the deposition parameters [4].

It was essential to use filtering on the dc-bias line, including low-frequency filtering which was found to reduce the noise-induced TLS energy fluctuations. Low-pass filters with cut-off frequencies of approximately 30 Hz were employed at room temperature and on the 3 K plate. A 3 dB microwave attenuator was installed on the 0.7 K plate to thermalize the center conductor of the coaxial cable carrying the dc voltage. Finally, a Cu-powder low-pass filter was used at the base (~ 10 mK) plate of the refrigerator.

The tunable micro- V resonator was measured at temperatures $T \leq 25$ mK in three separate cool-downs. In each cool-down, the bias voltage V_{bias} was swept over

a 60 mV range corresponding to $|E_{\text{bias}}| \leq 120$ kV/m within the capacitor bridge dielectric, while the microwave power was set such that the maximum time-averaged photon number on resonance was $\bar{n}_{\text{max}} \simeq 0.4$.

Figure 2(a) shows spectroscopy results from one of the cool-downs. The wide dark region corresponds to the cavity resonance perturbed by the TLSs. The large number of fine features crossing the cavity resonance ω_c are due to TLSs. Using a first analysis which neglects strong coupling effects, we directly analyze their energies; we fit the hyperbolic energy of the TLSs with $\Delta_0 \simeq \hbar\omega_c$ to Eq. 1. The fit to the observed TLSs from Fig. 2(a) are shown in Fig. 2(b), where each fit yields a Δ_0 , Δ and p_z for the corresponding TLS.

Assuming a representative distribution of TLSs from the double-well minima model with dipole moments that are not correlated with Δ_0 , the low-power loss tangent of the host dielectric from N TLSs is

$$\tan \delta_0 = \frac{\omega_c}{2\epsilon_0\epsilon_r BV} \frac{d_0}{\delta V_{\text{bias}}} \sum_{i=1}^N p_{z,i}, \quad (2)$$

where $\epsilon_0\epsilon_r$ is the permittivity of SiN_x , δV_{bias} is the bias voltage sweep range, and B is the measurement bandwidth estimated from the minimum and maximum resolved Δ_0 . A total of 60 hyperbolas were observed from the three separate cool-downs, from which Eq. 2 predicts $\tan \delta_0 = 7.8 \times 10^{-4}$.

The data of Fig. 2(a) contains 2001 distinct transmission curves $|S_{21,i}|$ (vertical traces), each taken at a unique V_{bias} . To obtain the ensemble-averaged response from many weakly coupled TLSs, we took the average of $|S_{21,i}|$, resulting in a Lorentzian resonance line-shape $|\bar{S}_{21}|$ (see inset of Fig. 3). A Lorentzian fit [24] determined that the TLS ensemble at $\bar{n}_{\text{max}} \simeq 0.4$ gives rise to $\tan \delta_e = 3.8 \times 10^{-4}$. However, we also found that this loss is reduced by a factor of 2 as compared to the lowest measurement power in a previous resonator made of SiN_x with a similar dielectric volume [25], such that the low-field loss tangent is actually $\tan \delta_{e,0} = 2 \tan \delta_e$. Therefore we find $\tan \delta_{e,0} \simeq \tan \delta_0$ or consistency between the loss from individual TLS and the ensemble average, such that the observations agree with a TLS-only model of loss. This type of check places constraints on new models which add complex strongly-interacting excitations [26].

The DWR spectroscopy gives a weighted distribution of dipole moments because the probability of observing a given p_z is proportional to the energy sweep range, which itself depends on p_z as described by Eq. 1. The unweighted distribution, shown in Fig. 3, is $\mathcal{N}(\bar{p}_{z,i}) = N_i \times p_{z,\text{max}}/\bar{p}_{z,i}$ where N_i is the count (observed in the DWR spectrum) of TLS moments in bin i , with center value $\bar{p}_{z,i}$.

TLSs with $p_z < 1$ Debye are undercounted as their coupling to the cavity is usually too small to be detectable.

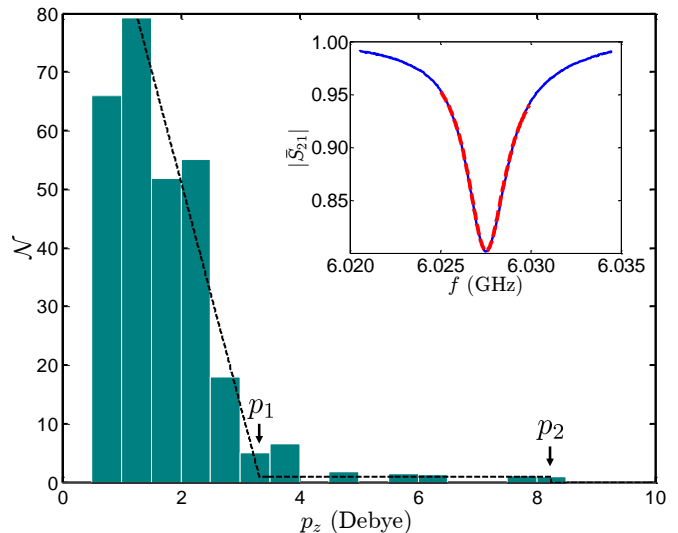


FIG. 3. TLS distribution of p_z obtained from hyperbolic trajectories ($\Delta_0 \cong \hbar\omega_c$) observed in three spectroscopy sweeps. Inset shows the average transmission $|\bar{S}_{21}|$ (blue) obtained from the data in Fig. 2 and optimum fit (red dashed curve) versus frequency f .

For TLSs with $p_z > 1$ Debye the histogram suggests at least two dipole types, one type with a large dipole size of $p_z \simeq 8$ Debye and another more numerous distribution below 4 Debye.

A fit to the measured distribution above 1 Debye was performed with two uniform distribution segments in p_z , and a linear transition between the two (see Fig. 3). The fit error was weighted according to the contribution of each bin to the loss tangent, which imposed a factor of p_z relative to the distribution \mathcal{N} (see Eq. 2). An optimum least-squares Monte Carlo (LSM) fit gave a uniform distribution (horizontal line) for the largest moment of $p_z = p_2 = 8.25$ Debye = 1.72 eÅ downward, where p_2 corresponds to the center of the rightmost bin containing TLSs. Therefore, this result is consistent with dipoles of $p \simeq 8.3$ Debye with a random distribution of angles. The transition region is encountered at $p_z = p_1 = 3.3$ Debye = 0.69 eÅ which continues all the way down to the lowest fit moment of 1 Debye. Since the fit did not find a uniform distribution below 3.3 Debye, it implies that the corresponding TLSs do not share the same dipole size p with a random angular distribution. The ability to resolve two (or more) dipole types in the film is created by uniformity of the dc electric field applied in the technique, while accuracy is created by the accuracy of the dc voltage. Previous TLS dipole moment measurements found an 8 Debye dipole from a different SiN_x film type [21], which is similar to p_2 but not p_1 . This technique should be repeated in the future for alumina to provide additional classifications to TLSs within.

Figure 4(a) shows a close-up of a DWR spectra which resolves a TLS with a stronger-than-average TLS-

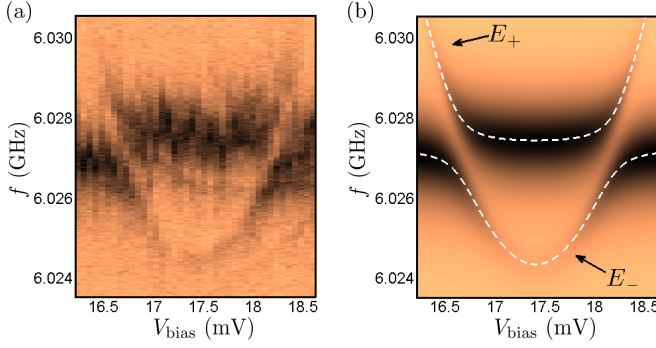


FIG. 4. (a) False-color plot of measured $|S_{21}|$ vs. frequency f and bias voltage V_{bias} showing avoided crossings due to an energy-tuned TLS with $\Delta_0 \cong \hbar\omega_c$. Data is taken at $T = 24$ mK and $\bar{n}_{\text{max}} \simeq 0.4$. Light copper and black correspond to $|S_{21}| = 0.60$ and $|S_{21}| = 0.43$, respectively. (b) Optimum fit to data using a CQED-based model. White dashed curves show the extracted low-power eigenenergies E_+ and E_- of the system.

resonator coupling. The CQED spectral line-shape for a fixed bias is known [25] and used with Eq. 1 to fit for the TLS and resonator parameters. Figure 4(b) shows the optimum fit to the spectra using the LSM method. The key extracted parameters were $\Delta_0/\hbar = 6.024540$ GHz, $g/2\pi = 753$ kHz, $p_z = 6.0$ Debye and $T_2 = 2/\gamma_{\text{TLS}} = 313$ ns where T_2 is the TLS coherence time assuming negligible dephasing. The coherent exchange is approximately as fast as the TLS relaxation ($g/\gamma_{\text{TLS}} = 0.74$) and similar to the resonator decoherence ($g/\kappa = 0.35$) where κ is the resonator photon decay rate from external coupling and other weakly coupled TLSs. The Jaynes-Cummings eigenenergies

$$E_{\pm} = \frac{1}{2} \hbar(\omega_c + \omega_{\text{TLS}}) \pm \hbar\sqrt{g^2 + (\delta/2)^2}, \quad (3)$$

where $\omega_{\text{TLS}} = \mathcal{E}'/\hbar$, and δ represents the TLS-resonator detuning, are shown by the white dashed curves in Fig. 4(b). The extracted value for p_z using the eigenenergies captures g and is therefore more accurate than the method used for Fig. 2(b). However, the difference is less than 1% in the extracted p_z , implying that the dipole distribution of Fig. 3 is not limited by the analysis technique for the present number of TLSs.

The fit parameters of this analysis also allow for a quantum mechanical measurement of the RMS vacuum field E_{RMS} . From the optimum fit parameters we calculate $E_{\text{RMS}} = \hbar g \mathcal{E}' / p_z \Delta_0 = 25$ V/m, while the resonator parameters give $E'_{\text{RMS}} = \hbar \sqrt{\omega_c / (2\epsilon_r \epsilon_0 \hbar V)} = 21$ (using $\epsilon_r = 6.5$ [4] and the bridge capacitors' dielectric volume V), a value which is 16% smaller than E_{RMS} . Since V was not underestimated and the individual p_z is very accurate, the small difference must be attributed to the uncertainty in g .

In summary, TLS spectroscopy in an insulating SiN_x film was achieved by coupling of TLSs to a linear super-

conducting resonator while TLS transition energies were tuned using an applied dc electric field. The analysis of 60 TLSs revealed at least two TLS dipole sizes; one kind showed a large spectral weight below 3.3 Debye, and one was consistent with a uniform angular distribution with a moment of 8.25 Debye.

The dipole moment distribution and other TLS parameters obtained from the DWR spectroscopy is viewed by the authors as a step towards better characterization of TLSs in insulating films. This study can be extended to any insulating amorphous solid to accurately measure multiple TLS dipole moments. The CQED measurement also allowed a self-consistency check with the standard model as well as the predicted vacuum fluctuations in this solid state system. Finally, knowing that TLSs with relatively long coherence times have been detected using CQED-based measurements and that the coupling can be increased further [12], this tunable technique might be extended to allow the use of TLSs as qubits.

The authors would like to thank Christopher Lobb, Ray Simmonds and Yaniv Rosen for many useful discussions.

-
- [1] J. M. Martinis, K. B. Cooper, R. McDermott, M. Steffen, M. Ansmann, K. D. Osborn, K. Cicak, S. Oh, D. P. Pappas, R. W. Simmonds, and C. C. Yu, Phys. Rev. Lett. **95**, 210503 (2005).
 - [2] J. Gao, J. Zmuidzinas, B. A. Mazin, H. G. LeDuc, and P. K. Day, Applied Physics Letters **90**, 102507 (2007).
 - [3] A. D. O'Connell, M. Ansmann, R. C. Bialczak, M. Hofheinz, N. Katz, E. Lucero, C. McKenney, M. Neeley, H. Wang, E. M. Weig, A. N. Cleland, and J. M. Martinis, Appl. Phys. Lett. **92**, 112903 (2008).
 - [4] H. Paik and K. D. Osborn, Applied Physics Letters **96**, 072505 (2010).
 - [5] S. Oh, K. Cicak, J. S. Kline, M. A. Sillanpää, K. D. Osborn, J. D. Whittaker, R. W. Simmonds, and D. P. Pappas, Phys. Rev. B **74**, 100502 (2006).
 - [6] Z. Kim, V. Zaretskey, Y. Yoon, J. F. Schneiderman, M. D. Shaw, P. M. Echternach, F. C. Wellstood, and B. S. Palmer, Phys. Rev. B **78**, 144506 (2008).
 - [7] M. R. Vissers, J. Gao, D. S. Wisbey, D. A. Hite, C. C. Tsuei, A. D. Corcoles, M. Steffen, and D. P. Pappas, Applied Physics Letters **97**, 232509 (2010).
 - [8] C. Deng, M. Otto, and A. Lupascu, Journal of Applied Physics **114**, 054504 (2013).
 - [9] R. W. Simmonds, K. M. Lang, D. A. Hite, S. Nam, D. P. Pappas, and J. M. Martinis, Phys. Rev. Lett. **93**, 077003 (2004).
 - [10] Y. Shalibo, Y. Roife, D. Shwa, F. Zeides, M. Neeley, J. M. Martinis, and N. Katz, Phys. Rev. Lett. **105**, 177001 (2010).
 - [11] M. Neeley, M. Ansmann, R. C. Bialczak, M. Hofheinz, N. Katz, E. Lucero, A. O'Connell, H. Wang, A. N. Cleland, and J. M. Martinis, Nature Physics **4**, 523 (2008).
 - [12] B. Sarabi, A. N. Ramanayaka, A. L. Burin, F. C. Wellstood, and K. D. Osborn, arXiv preprint arXiv:

- 1405.0264v2 (2014).
- [13] A. M. Holder, K. D. Osborn, C. J. Lobb, and C. B. Musgrave, Phys. Rev. Lett. **111**, 065901 (2013).
 - [14] L. Gordon, H. Abu-Farsakh, A. Janotti, and C. G. Van de Walle, Scientific reports **4** (2014).
 - [15] W. A. Phillips, Journal of Low Temperature Physics **7**, 351 (1972).
 - [16] P. W. Anderson, B. I. Halperin, and C. M. Varma, Philosophical Magazine **25**, 1 (1972).
 - [17] P. W. Anderson, Ill-Condensed Matter/La Matiere Mal Condensee, 31 st Session of the Les Houches Summer School , 159 (1978).
 - [18] A. Lupaşcu, P. Bertet, E. F. C. Driessen, C. J. P. M. Harmans, and J. E. Mooij, Phys. Rev. B **80**, 172506 (2009).
 - [19] J. H. Cole, C. Mller, P. Bushev, G. J. Grabovskij, J. Lisenfeld, A. Lukashenko, A. V. Ustinov, and A. Shnirman, Applied Physics Letters **97**, 252501 (2010).
 - [20] M. J. A. Stoutimore, M. S. Khalil, C. J. Lobb, and K. D. Osborn, Applied Physics Letters **101**, 062602 (2012).
 - [21] M. S. Khalil, S. Gladchenko, M. J. A. Stoutimore, F. C. Wellstood, A. L. Burin, and K. D. Osborn, Phys. Rev. B **90**, 100201 (2014).
 - [22] B. Golding, M. v. Schickfus, S. Hunklinger, and K. Dransfeld, Phys. Rev. Lett. **43**, 1817 (1979).
 - [23] G. J. Grabovskij, T. Peichl, J. Lisenfeld, G. Weiss, and A. V. Ustinov, Science **338**, 232 (2012).
 - [24] M. S. Khalil, M. J. A. Stoutimore, F. C. Wellstood, and K. D. Osborn, Journal of Applied Physics **111**, 054510 (2012).
 - [25] B. Sarabi, *Cavity quantum electrodynamics of nanoscale two-level systems*, Ph.D. thesis, University of Maryland - College Park (2014).
 - [26] L. Faoro and L. B. Ioffe, arXiv:1404.2410 (2014).